

## **Synthesis of Engineering Decisions with an Evolving Feasible Space**

Liang Zhu and David Kazmer

Department of Mech. and Ind. Engineering

University of Massachusetts Amherst

### **Abstract**

A methodology is presented to assist the synthesis of engineering decisions based on the representation of feasible space. Given a parametric model and initial specifications, the Extensive Simplex Method is proposed to traverse the extreme points of an approximate linear model. The connected extreme points are projected to a set of two-dimensional viewing planes to visualize the feasible space. Based on the established bounds of the feasible space, the designer can assess the system performance capability, evaluate the feasibility of design alternatives, negotiate the trade-off of system performance attributes, and eventually converge to a desirable engineering design. The method is applied to a beam design problem throughout the design process of concept selection, parametric design refinement, and inverse reasoning. The result indicates that the proposed methodology can help the designer not only to obtain a flexible design solution with better overall system performance, but also to gain insight to the design problem and its specifications. Such insight into the problem leads to increased competence in product design.

### **Keywords**

Engineering Decision Making, Multiple Objectives, Feasible Space, Extensive Simplex Method

## **1 Introduction**

Engineering design involves a set of decisions that are made throughout a design process, where a decision can be viewed as an irrevocable allocation of resources and a choice taken from a set of options [1]. Starting with initial product specifications, the designer decides appropriate configurations to satisfy the specifications. During this iterative process, the designer accumulates the understanding of the design problem and eventually comes to the final solution with a desirable level of cost, risk, and other

performance attributes. As modern engineering practices strives to increase productivity through reduced product development times, reduced tooling costs, reduced energy consumption, efficient material utilization, and increased processing yields, the design objectives represent an extremely complex set of constraints that are seldom concurrently satisfied. The final design decision is always the result of a tradeoff between multiple attributes. It is not trivial to discover the tradeoff relationships between multiple attributes. Any single function that explicitly combines the attributes with different weight factors rarely gives the satisfied optimal solution. Plus, the pure mathematical optimization provides few insights to the physics of the problem, and little understanding for the designer. As such, it is necessary to develop a solid methodology to support the synthesis of engineering decisions throughout design process, from initial concept exploration through final detailed design and manufacturing.

The formal theory of decision making has been well established in Economic Management [2, 3]. In the business model, multiple attributes are generally transformed into the equivalents of the cost to obtain the maximum profit. More extensively, the utility instead of the cost can be formulated to evaluate the trade-off of multiple attributes through a set of lottery equivalencies. Reflecting on the community of engineering design research, the decision-related design methodologies seek to maximize the value of the design by system characterization and parameter selection. For instance, Antonsson and Otto presented a method based on the mathematics of fuzzy sets to model the imprecision of design, so that the designer could evaluate the design options under uncertainty [4]. Bras and Mistree discussed a compromise decision support problem to perform both axiomatic and robust design [5]. Utility theory was also applied to engineering design where the design goal is to maximize the overall utility of multi-attributes in a multiplicative form [6]. Given the simplicity of utility function formulation, the utility-based approach has been fairly adopted in some research works [7-9]. While the above methods facilitated the paradigm of engineering design as a decision making process, these approaches focused mainly on the final evaluation of design options and did not provide significant assistance in the synthesis of design decisions throughout design process, e.g., the justification of initial specifications, the configuration refinement to satisfy the specifications, and the convergence towards a final set of design decisions.

Some researches have established graphical design representations to facilitate the decision process of engineering design. Rinderle et al proposed the interactive manipulation of the design parameters and behaviors [10]. Ulrich et al developed a designer's spreadsheet to propagate design changes via constraint perturbation [11]. Cagan et al presented a design methodology for the adaptive generation and selection of design alternatives [12]. The interval representation was also applied to analyze the tolerance behavior under uncertain variations [13, 14]. Overall, these research efforts have provided tools that promote and assist an interactive design process and provide relative design information for making design decisions. As capable, autonomous, artificial intelligent design technology will not be available in the foreseeable future, these tools are useful for providing a human decision maker with a continuous stream of information for synthesis of design options.

This paper discusses a design methodology that facilitates the synthesis of design decisions throughout an interactive design process via the visualization of an evolving feasible space. Given a parametric model between the design parameters and performance attributes, the feasible space that satisfies all initial specifications is solved by the Extensive Simplex Method. The decision makers can then justify the feasibility of the design model, explore and refine the design behavior, relax or tighten the specifications, and eventually converge to a desired solution. The paper proceeds as follows. First, a brief introduction on the Extensive Simplex Method is given in Section 2. A formal discussion of design synthesis with an evolving feasible space is followed in Section 3. The methodology is then applied to a simple case study, a beam design problem, to demonstrate the utility and potential of the approach.

## 2 Solving the Feasible Space

Consider an engineering decision problem with the design parameters  $x_i$  to satisfy the specifications of the performance attributes  $y_j$  as follows:

$$LSL_j \leq y_j \leq USL_j \quad (j = 1, 2, \dots, m), \quad (1)$$

and

$$y_j = f_j(x_1, x_2, \dots, x_n),$$

$$LCL_i \leq x_i \leq UCL_i \quad (i = 1, 2, \dots, n).$$

where  $LCL_i$  and  $UCL_i$  are respectively the allowable lower and upper control limits of  $x_i$ ,  $LSL_j$  and  $USL_j$  are the lower and upper specification limits of  $y_j$ . Without the loss of

generality, single-side design parameters and performance attributes can also be expressed in the form of Equation (1) with  $-\infty$  or  $+\infty$  limits.

Supposing that the performance attributes  $y_j$  are coupled and competitive with each other (e.g., time, cost, and reliability), it is not trivial to satisfy all specifications and achieve a desired solution at the same time. One conventional approach is to define an objective function and find a design solution with the minimized (or maximized) performance value. However, such an ‘optimal’ objective function, which truly reflects the preference of the designer, is often unknown and confounded with conflicting performance attributes. The common practice of multiplying or adding the attributes with defined weighting factors rarely results in a satisfactory solution. As such, it is valuable to first explore the feasible space constituted by Equation (1) without any preference assumptions. Once the practitioner acquires the efficient frontier for multiple attributes, the preferred decisions can be selected for compromising these attributes. As the efficient but generic solution of the feasible space for a system nonlinear equations is yet impossible, an Extensive Simplex Method was developed to efficiently solve the feasible space of linear equations [15]. A nonlinear model may be approximated as a set of piecewise linear segments to assemble the non-linear and even non-convex feasible space. While linear approximation is certainly not trivial in complicated nonlinear problems, it is not the focus of this paper. The reader is referred to some capable approximation methods described elsewhere [16, 17].

Let the performance attributes  $y_j$  be approximated as a linear function of design parameters  $x_i$ ,  $y_j = \alpha_{j1}x_1 + \alpha_{j2}x_2 + \dots + \alpha_{jn}x_n$ . Equation (1) is then approximated as:

$$LSL_1 \leq \alpha_{11}x_1 + \alpha_{12}x_2 + \dots + \alpha_{1n}x_n \leq USL_j \quad (2)$$

...

$$LSL_m \leq \alpha_{m1}x_1 + \alpha_{m2}x_2 + \dots + \alpha_{mn}x_n \leq USL_m$$

with the constraints  $LCL_1 \leq x_1 \leq UCL_1, \dots, LCL_n \leq x_n \leq UCL_n$ .

The above equation can be transformed to generic form:

$$a_{11}x_1 + a_{12}x_2 + \dots + a_{1n}x_n \leq b_1, \quad (3)$$

...

$$a_{m1}x_1 + a_{m2}x_2 + \dots + a_{mn}x_n \leq b_m.$$

Each line in Equation (3) represents one constraint in an  $n$ -dimensional Euclidean space where  $n$  is the number of design parameters. Every constraint separates the space into two regions. One region represents the feasible space that satisfies this constraint, another region is the infeasible space. Combining all constraints together, we have a hyper-dimensional polyhedron  $\mathbf{P}_X$  representing the feasible space of design parameter in Equation (3). Each vertex of the polyhedron is the intersection point of at least  $n$  constraints, known as an extreme point. The polyhedron can be defined by all extreme points and their topological connections. It is easy to deduce that the polyhedron is convex given all linear constraints [18]. Moreover, the polyhedron  $\mathbf{P}_X$  in the primal space can be mapped to the dual space in order to trace the feasible space of all performance attributes. Supposing each point in the primal space represents a set of design parameters and the point in the dual space represents a set of attribute values, each extreme point in the primal space determines a point in the dual space. Therefore, the feasible space can also be represented by a polyhedron  $\mathbf{P}_Y$  in an  $m$ -dimensional Euclidean space, where  $m$  is the number of performance attributes. The vertex of  $\mathbf{P}_Y$  is decided by the correspondent performance values of the extreme point in the primal polyhedron  $\mathbf{P}_X$ .

As such, the Extensive Simplex Method is developed to solve the extreme points of Equation (3). The feasible design space (primal space) is defined by the parameter values of these extreme points, and the feasible performance space (dual space) is determined by the performance values of the extreme points. It should be noted that the algorithm is related to the research of Multiple Objective Linear Programming (MOLP) [19, 20]. However, the Extensive Simplex Method explores the entire topological structure of the global feasible space to assist the interactive engineering design process, while the MOLP looks for the optimal solutions for specified attributes. As a result, the algorithm is designed and implemented differently.

The algorithm uses a graph data structure  $\mathbf{G}$  to store the extreme points. Let the first extreme point  $X^e$  be the intersection point of  $n$  active constraints, i.e., the solution of  $n$  equations in Equation (2). The neighbor nodes of  $X^e$  can be found by substituting one constraint in the set of  $n$  active constraints, an operation called pivoting. It is worth noting that every combination of  $n$  constraints does not result in an extreme point. An effective mechanism for selecting the entering and leaving constraints for the pivoting operation

has been developed and tested under different scenarios including degeneracy and cycling [15]. The demonstrative flowchart of the Extensive Simplex Method is shown in Figure 1. The algorithm starts with the first extreme point that can be identified by a two-step linear optimization problem [18]. For each leaving constraint labeled  $r$ , the modified lexicographic rule is applied to locate the correspondent entering constraint labeled  $k$ . A new extreme point  $X^{new}$  is then generated and added into the graph  $G$  until no more pivoting is required. In the end, all extreme points and their connections are saved in the vertex list of the graph  $G$ .

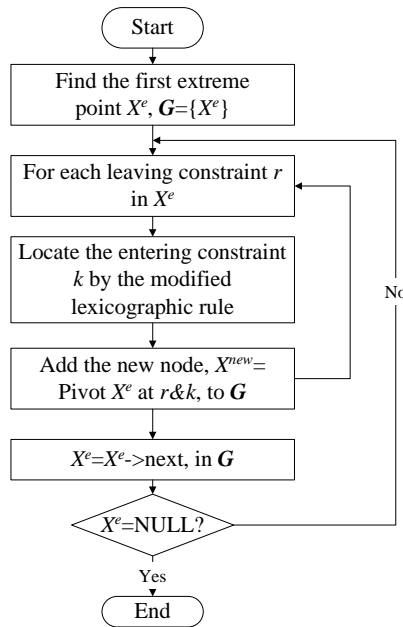


Figure 1: The flowchart of the Extensive Simplex Method

### 3 Design Process with Feasible Space

In order to exhibit the feasible space, the hyper-dimensional polyhedron must be visualized to the human designer. Some researchers have focused on projecting high-dimension data onto a two-dimensional screen [21, 22]. Because there is only one two-dimensional screen to display all multivariate data, the plot is oriented in a specialized coordination reference frame. This approach not only ignores most topological connections of the data, but also impedes the interactive manipulation of multivariate vectors. Furnas et al discussed a method that utilizes the composition of projections and sections to display high-dimensional objects at any intermediate dimension [23]. This

paper adopts these two general graphical techniques, projection and section, to construct views of the hyper-dimensional polyhedron.

Suppose a beam design problem with three design parameters (e.g., length, height, and width) and two performance attributes (e.g. product cost and failure risk). Assuming a parametric model between design parameters and performance attributes, the feasible space of design model can be established from the Extensive Simplex Method. The visualization of the feasible design space is shown in Figure 2. In this case, the feasible design space is a three-dimensional polyhedron. The polyhedron can be projected to three orthogonal two-dimensional viewing planes, named  $x_1x_2$ ,  $x_2x_3$ , and  $x_3x_1$ . The current design vector is shown as the intersection point of three dashed lines. In order to locate the design vector relative to the boundary of the feasible space, a section view is taken with a plane parallel to  $x_1x_2$  at the current design point. The intersection shape is copied to the plane  $x_1x_2$ . Similarly, the section view is applied to the direction of  $x_2x_3$  and  $x_3x_1$  at the current design point. The intersection shape is recorded in the correspondent plane. As such, the projection provides a static picture of the hyper-dimensional polyhedron, and the section reveals the dynamic changes of current design vector relevant to the feasible space. According to Figure 2, an infeasible design vector may be outside the polyhedron in three-dimensional feasible space, but still projected inside the boundary in all three projection view. However, an infeasible design vector must be outside the feasible boundary in at least one section view. This is an important feature of the interface as to justifying the feasibility of design solution.

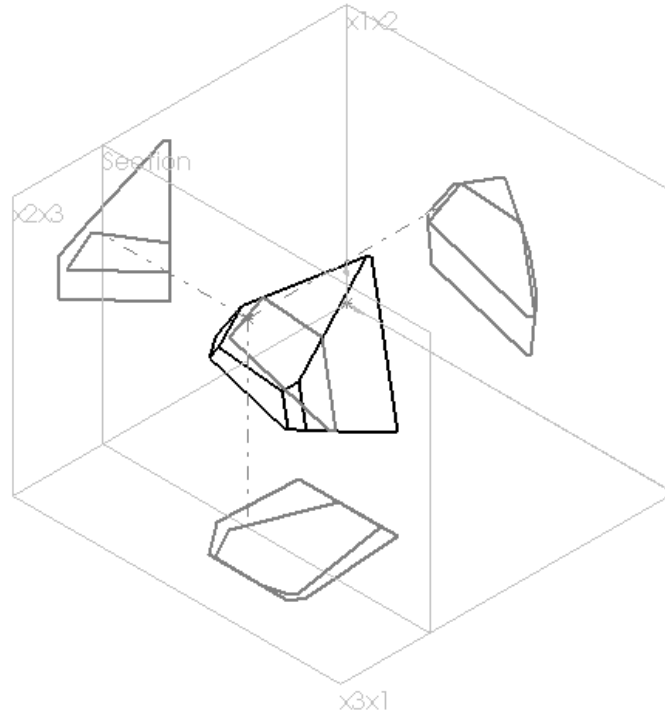


Figure 2: Projection and Section in a Three-Dimensional Design Space

The concept can be extended to the  $n$ -dimensional space. A layout of the general interface is shown in Figure 3, composed of three main components corresponding to the design parameters and performance attributes. They are the function matrix, the design space, and the performance space, labeled I, II, and III. The function matrix illustrates the system relations between the design parameters and the performance attributes, where each column represents one design parameter and each row represents one performance attribute. On the other hand, every two design parameters comprise a two-dimensional plane. All planes together comprise the entire design space. The projection and section views of the hyper-dimensional polyhedron are displayed on these two-dimensional planes. For instance, the plane of  $x_3x_1$  is zoomed in Figure 3. The projection of feasible space is shaded with light color, labeled ①. And the section of feasible space is shaded with dark color, labeled ②. For the convenience of expression, the projection and section regions in the two-dimensional plane are named as the global space and local space. The current design vector, labeled ③, is identified by the crossed hairlines in the two-dimensional plane. Based on the feasible region identifies in the global and local spaces, the designer can interactively adjust the parameter values of design vector. The performance space is organized in a similar manner.

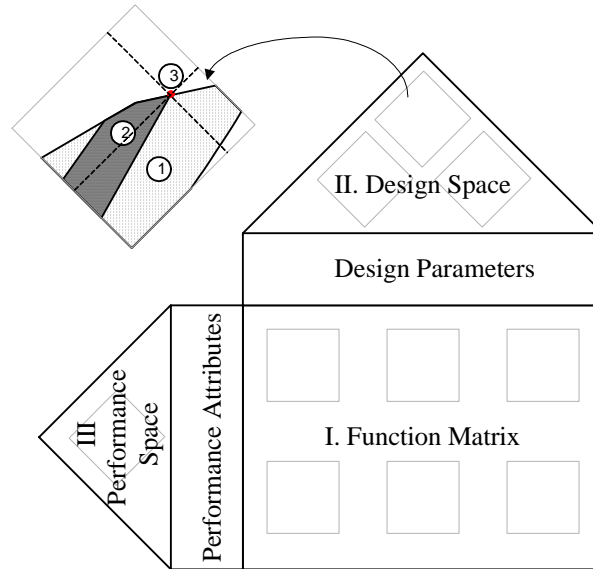


Figure 3: The Layout of Design Interface with Feasible Space

With the general interface established as in Figure 3, various design decisions can be made based on the representation of feasible space, e.g., concept selection, design refinement, and inverse reasoning.

### 3.1 Concept Selection

Conceptual design is one of the most important stages of design process. Given the design requirements, many concept designs can be quickly generated through brainstorming and other inventive methods. Some of these concepts may be quickly eliminated by estimating the technical feasibility with respect to power, cost, or size. On the other hand, more than one concept may seem appropriate for further development towards the final solution. Due to the severe cost and time constraints in engineering practice, one concept is often chosen over other alternatives for further development. In this case, the decision of concept selection will directly affect the final capability of the product design.

The described representation of an evolving feasible space can investigate the potential of the design configurations, identify the dominant constraints of the system performance, and provide suggestions for possible changes. The feasible space derived from the Extensive Simplex Method is the main evaluation basis of concept selection here. Since the design alternatives may have different model topologies and therefore

different sets of design parameters, it is unreasonable to compare the design spaces of different design alternatives. Instead, because most design configurations have the same or at least comparable performance attributes, the performance space can be used to compare different design concepts.

The Pareto optimal boundary is an important measure of possible design performance when the design objective is to improve the system performance. The term "Pareto optimal" here means that there is no way to improve one performance attribute without deteriorating other performance attributes [24]. All Pareto optimal solutions combine to a set, called Pareto optimal set. The Pareto optimal set can be located on the boundary of feasible space in the presented design interface.

Consider the following example in which there are two proposed design concepts for a beam design. The first design has an I-shape cross section and the second has a box-shape cross section. These two configurations have different design parameters. However, they both can be measured by the performance attributes of product cost and failure risk. Therefore, each concept can generate a feasible performance space with respect to cost and risk. In this case with two performance attributes, the feasible performance space is a two-dimensional polygon. Suppose the feasible performance space of the I-beam design is the polygon  $ABCDE$  with five extreme points, and the feasible performance space of the box-beam is the polygon  $1234$  with four extreme points. Three possible scenarios of two feasible performance spaces are shown in Figure 4. Assuming the designer prefers lower product cost and lower failure risk, the Pareto optimal set is the lower-left boundary of the feasible performance space, labeled  $123$  and  $CDE$  respectively for two concepts in Figure 4. In the situation (a), the polygon  $ABCDE$  is totally included in the polygon  $1234$ , which means that all possible performance values of the I-beam design are a subset of the box-beam design. Thus, the concept of box-beam is chosen. The situation (b) is slightly different. Two performance spaces are exclusive to each other. However, the Pareto optimal boundary  $123$  of the box-beam design is superior to the Pareto optimal boundary  $CDE$  of the I-beam design. Again, the box-beam is considered a better design than the I-beam concept in term of the performance of cost and risk. The last situation (c) has two intersecting performance spaces. Each design concept exhibits its own advantages over different performance ranges. Therefore, the

decision should be based on the relative importance of two performance attributes. For instance, a designer with a preference for lower cost may select the I-beam concept, where as a designer with a preference for lower risk may select the box-beam concept. Alternatively, since the feasible space is bounded by the specifications, the designer may refine the specifications in the situation (c) to obtain an unambiguous concept selection.

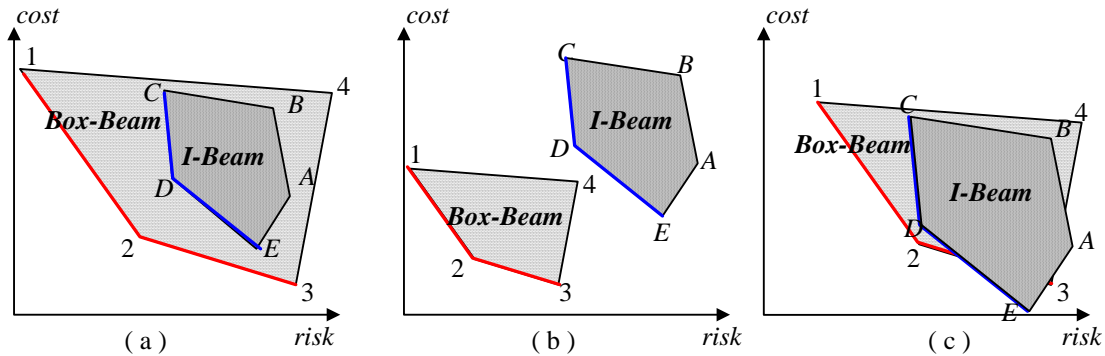


Figure 4: Three Possible Scenarios of Performance Space Comparison

It should be noted that the mean system performance is not always the only concern, even when all specifications are satisfied. Such examples are common in quality engineering. For instance, Taguchi's method seeks the most robust design by minimizing the performance variation caused by uncontrolled noise [25, 26]. Reflecting on the decision making with feasible space, the flexibility of the system configuration instead of the Pareto optimal boundary should be compared. The flexibility provides a measure of the adaptability of the system while maintaining all performance attributes within specifications [27]. In the representation of feasible space, the flexibility can be represented by the size of the global space. The larger global space means the greater capability of the system to maintain the feasibility under uncontrolled variation. Depending on the design preferences, the appropriate decision can be made based on the size and position of the configuration's global space.

### 3.2 Design Refinement

Once a concept has been chosen, the design process proceeds to the design refinement stage. The goal of the design refinement is to adjust the values of design parameters and obtain the optimum overall system performance. Some researches utilize fuzzy set to represent the acceptable regions of the design and performance in order to

successively refine the design configuration [4]. In this paper, the representation of feasible space is used to reason the common design questions, e.g.: 1) whether the current design is feasible; 2) how to improve the infeasible design; and 3) how to negotiate the tradeoff of the system performance.

The design feasibility can be achieved using the design space. Figure 5 provides an example of feasibility evaluation in the two-dimensional plane of  $x_1x_2$ . Suppose that the dark shadowed region is the local design space and the light shadowed region is the global design space. The current design vector  $X^C=(x_1^C, x_2^C, \dots, x_n^C)$  is located outside the local design space, so  $X^C$  is an infeasible design. In order to achieve a feasible design, the designer may consider decreasing the value of the design parameter  $x_2$  to produce a feasible design  $X'$  as indicated by the dashed line in Figure 5 (a). On the other hand, the local design space of  $x_1x_2$  is dependent on other parameters. The modification of other parameters could change the position and size of the local space in Figure 5 (b). In fact, any point inside the global design space of  $x_1x_2$  is theoretically reachable with some adjustments of other parameters. The adjustment of  $x_1$  and  $x_2$  in Figure 5 will not change the local space in this observation window, but will enlarge/shrink/move the local space in other two-dimensional section views. In the case of Figure 5 (b), the values of  $x_1$  and  $x_2$  are maintained but other parameters are changed to achieve a feasible design  $X^C=(x_1^C, x_2^C, x_3, x_4, \dots, x_n)$ , in which the point  $(x_1^C, x_2^C)$  is inside the updated local space of the plane  $x_1x_2$ .

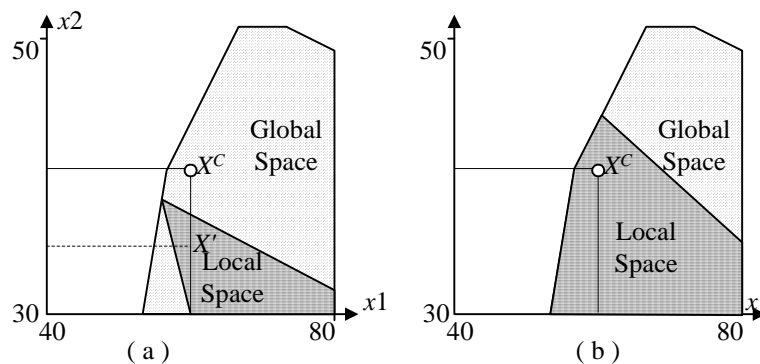


Figure 5: Feasibility and Flexibility in the Design Space

A feasible design is not necessarily the final design solution. The design is expected to exhibit an optimal performance trade-off, which requires the consideration of the Pareto optimal set in the performance space. An example of the performance space

for the beam design is shown in Figure 6. Note that the local performance space has been shrunk to a very small dark-shaded region around the current design vector while the global performance space is defined as a light-shaded polygon. The Pareto optimal boundary is the lower-left edge of the global performance space, assuming lower cost and risk are preferred. The effect of the design parameters on cost and risk are shown as the arrows. Suppose that there are four design parameters in total, each labeled vector corresponds to one design parameter. The intersection point is the current design vector  $X^C=(x_1^C, x_2^C, x_3^C, x_4^C)$ . The direction of the arrow represents the increasing direction of the design parameter. In addition, the starting point of the arrow is the performance with the lower control limit of the correspondent parameter, and the ending point is the performance with the upper control limit. For instance, the point  $U$  represents the performance of the design vector  $X=(LCL_1, x_2^C, x_3^C, x_4^C)$ , and the point  $V$  represents the performance of  $X=(UCL_1, x_2^C, x_3^C, x_4^C)$ . As such, the Pareto optimal boundary provides the feasible trade-off of the system performance, while the arrows indicate how to adjust the design parameters and achieve the desired performance values. In the case of Figure 6, the designer may choose to decrease  $x_3$  and increase  $x_1$  to achieve a Pareto optimal design configuration. On the other hand, within the Pareto optimal set, decreasing  $x_2$  and  $x_4$  will likely yield the low cost beam design that suffers relatively high failure risk.

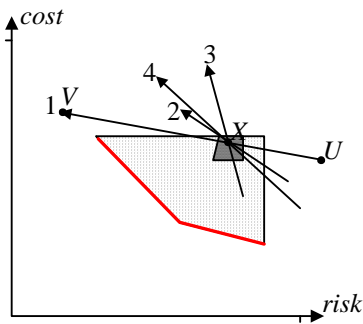


Figure 6: Design Sensitivity in the Performance Space

The design may be completed with an acceptable Pareto optimal solution if the specification was correctly defined. In practice, the final design rarely occurs in the first iteration. An inverse reasoning process is then desirable in order to develop the final specification and design solution.

### 3.3 Inverse Reasoning

During the design refinement, adjustments are made to the design parameters. Since the performance attributes are the direct concerns of the customer, there is significant desire to directly manipulate the performance attributes during product design. Corresponding to the manipulated performance levels, the design configuration has to be updated to reflect the change of the performance attributes. Such a process is defined here as inverse reasoning.

The inverse reasoning approach seeks to find the best solution for the specified performance through the steps of constraint propagation [28]. Through the use of the Extensive Simplex Method, the global feasible space provides the set of all design solutions that fulfill any specified level of system performance. The set of solutions is exhibited as the global design and performance space such that the designer can select the appropriate configuration corresponding to the system performance. Mathematically, suppose that the  $j$ -th performance attribute is maintained at the constant  $a$ , then the problem is equivalent to resolve the following model:

$$\begin{aligned} LSL_j &\leq y_j \leq USL_j, \quad \forall j \neq k & (4) \\ y_j &= a, \quad \forall j = k \\ LCL_i &\leq x_i \leq UCL_i, \quad \forall i \end{aligned}$$

As such, inverse reasoning in the design process can be solved by reapplying the Extensive Simplex Method with the above model in which equality constraints are applied to the performance attributes. It should be emphasized that the narrowing of one performance attribute may still generate a large set of feasible solutions. In order to narrow the selection, the designer has to successively narrow the desired ranges or values of other performance attributes until the design and performance space are eventually tightened to a single optimal design. An example of this process is shown in Figure 7. The lower-left side of the global space (a) is bounded by the specification limit of  $x_1$  and  $y_3$ . Assuming that the upper specification limit on  $y_3$  is reduced, the global space of  $y_1$ - $y_2$  is shrunk to the smaller region (b). Similarly, the reduction of the USL for  $y_1$  can eventually lead to a very small performance space (c). Although not shown in the figure, the design space also exhibits similar shrinkage. Therefore, the interested design configuration is clearly defined in the remaining design space.

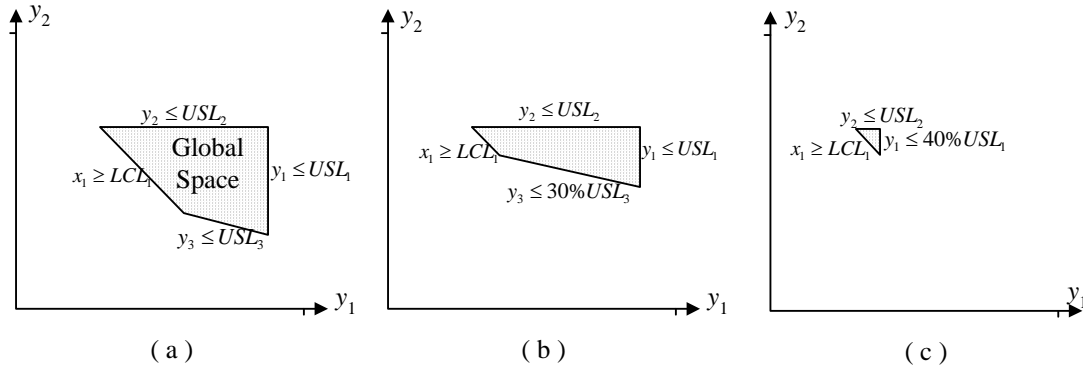


Figure 7: Global Space Change in Inverse Reasoning

It should be noted that the feasible space will shrink with the tightening of specifications. This behavior does not conflict with the philosophy of preserving design flexibility. During the concept selection stage, there is little understanding of the design problem. Therefore, extensive flexibility is desired to include broad ranges of performance for the design model. Once the concept is selected and more insight into the problem is revealed, the design configuration is then refined to a smaller region until the designer eventually obtains a satisfied solution -- a point. Such a step-by-step approach is interestingly analogical to the human design process. In addition, the process is entirely reversible, providing strong consistency with system development.

#### 4 Case Study

Beam design has been widely used as an engineering problem to demonstrate multi-attribute design methods. A schematic picture of a beam structure with two design configurations is shown in Figure 8. The application is part of an airframe design with the cyclic loading  $P$  and  $Q$ . The permissible maximum stress of the material corresponding to  $10^7$  cycles,  $\sigma_{per}$ , equals 124MPa, and its Young's modulus,  $E$ , equals 72.4GPa.

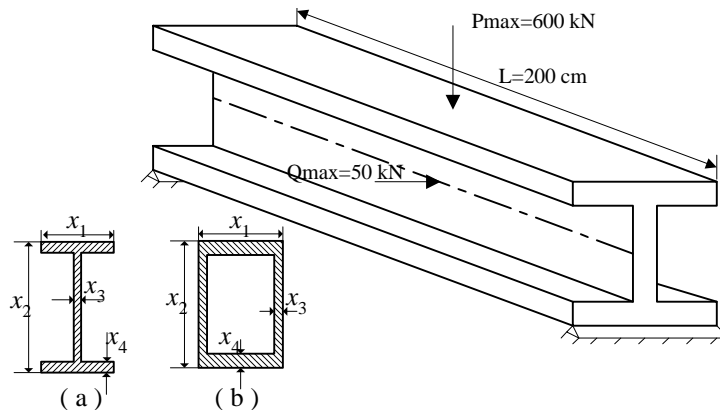


Figure 8: Beam Design

Figure 8 shows the design parameters of two configurations corresponding to (a) I-shape and (b) box-shape beams. The structures are symmetric, i.e. the top thickness is equal to the bottom thickness. Without any analysis or additional assistance, it is difficult to tell which configuration better satisfies the design requirements. According to the previous discussion, the evolving feasible space can be used to compare and develop the system designs. In terms of the performance attributes, two sets of metrics are formulated. A typical set of engineering metrics includes the area  $A$ , the deflection  $D$ , and the stress  $\sigma_{max}$  [29]. Another business-oriented approach may consider the product profit  $IRR$  and failure risk  $F$  based on the airframe economics and fracture mechanics [30]. Mathematically, for the I-shape beam design, we have:

$$A = 2x_2 x_4 + x_3 (x_1 - 2x_4) \leq 400 \text{ cm}^2 \quad (5)$$

$$D = \frac{165746}{x_3(x_1 - 2x_4)^3 + 2x_2 x_4 [4x_4^2 + 3x_1(x_1 - 2x_4)]} \leq 0.06 \text{ cm}$$

$$\sigma_{max} = \frac{150000x_2}{(x_1 - 2x_4)x_3^3 + 2x_4x_2^3} + \frac{1800000x_1}{x_3(x_1 - 2x_4)^3 + 2x_2 \cdot x_4(4x_4^2 + 3x_1(x_1 - 2x_4))} \leq 124 \text{ Mpa}$$

$$F = 1 - e^{-1.395 \cdot 10^{-26} A \cdot \sigma_{max}^{10}} \leq 10^{-3}$$

$$IRR = 1.417 - 3.049 \cdot 10^{-3} A - 6.822 \cdot 10^{-12} A \cdot e^{3.879 + 0.894 \tan(\frac{305 - \sigma_{max}}{140})} \geq 10\%$$

The initial specifications in the above equations are derived from the customer's needs and relative improvements over prior products. In addition, suppose the geometric constraints of the design parameters are:  $30\text{cm} \leq x_1 \leq 80\text{cm}$ ,  $30\text{cm} \leq x_2 \leq 50\text{cm}$ ,  $0.9\text{cm} \leq x_3 \leq 5\text{cm}$ ,  $0.9\text{cm} \leq x_4 \leq 5\text{cm}$ . (Although the two concepts coincidentally share the same geometric constraints in this example, this similarity should not be considered as a necessary condition for concept selection and other applications)

Note that the deflection and stress functions of Equation (4) exhibit significant non-linearity even in the defined small design domain. The direct linearization only approximate the model to 60% R-square, i.e., only 60% of design behavior can be effectively explained with a linear model. Therefore, the piecewise linear model is utilized. In this case, three segments on  $x_1$  and two segments on other parameters can bring the minimum R-square of three performance attributes (deflection) up to 86%,

while more segments does not significantly improve the R-square but continues to increase the system complexity. Therefore, the accepted piecewise linear model is:

$$\begin{bmatrix} A \\ D \\ \sigma_{\max} \end{bmatrix} = \begin{bmatrix} -525.690 & 5.900 & 5.900 & 98.200 & 68.2 & 0.000 & 0.000 & 0.000 & 0.000 & 0.000 \\ 0.564 & -0.007 & -0.003 & -0.026 & -0.017 & 0.004 & 0.002 & 0.001 & 0.018 & 0.011 \\ 199.169 & -1.359 & -1.295 & -13.531 & -9.754 & 0.421 & 0.461 & 0.515 & 9.154 & 6.300 \end{bmatrix} \begin{bmatrix} 1 \\ x_1 \\ x_2 \\ x_3 \\ x_4 \\ x_5 \\ x_6 \\ x_7 \\ x_8 \\ x_9 \end{bmatrix} \quad (6)$$

Where  $x_5 = 0$  if  $x_1 \leq 40$ , otherwise 1  
 $x_6 = 0$  if  $x_1 \leq 50$ , otherwise 1  
 $x_7 = 0$  if  $x_2 \leq 40$ , otherwise 1  
 $x_8 = 0$  if  $x_3 \leq 2$ , otherwise 1  
 $x_9 = 0$  if  $x_4 \leq 2$ , otherwise 1

As such, the global space can be assembled from 24 piecewise linear segments. The similar approach can be applied to the profit and risk functions. It is worth noting that the logarithm value of the risk is evaluated in order to provide a better approximation.

First, the global performance space of area, deflection, and stress are shown in Figure 9. The design concepts *a* and *b* are labeled in each window, corresponding to the I-beam and box-beam design. Because all three performance attributes are "smaller-better", the Pareto optimal set resides on the highlighted lower-left boundary of the global performance space. According to the graph of area versus deflection, the concept *a* provides better performance. However, the graph of area versus stress suggests that the concept *b* could be better for lower stresses. In other words, this comparison is matched to the third situation (c) of Figure 4. Therefore, further investigation is required in order to decide which concept is more likely to provide the desired system behavior.

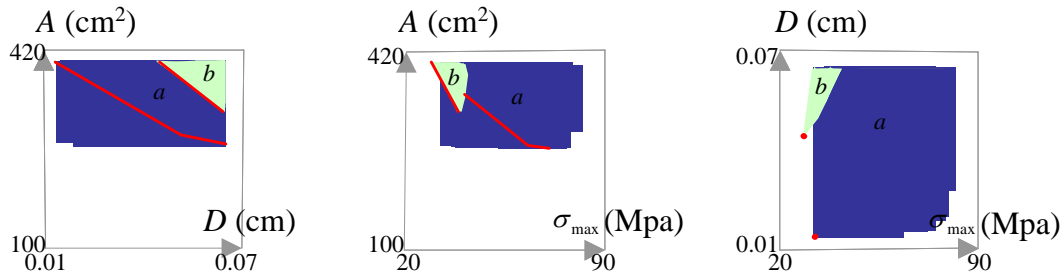


Figure 9: Concept Comparison with the Performance of Area, Deflection and Stress

The global performance space of profit  $IRR$  versus risk  $F$  is shown in Figure 10. Because higher profit and lower risk of the beam design is desired, the Pareto optimal set is on the upper-left boundary of the space. As illustrated in the figure, the Pareto optimal set of the concept  $b$  dominates that of the concept  $a$ . Therefore, the concept of box-beam is selected due to its potential to generate improved performance.

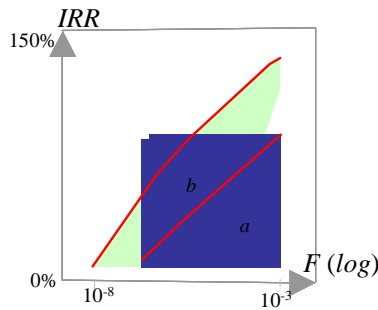


Figure 10: Concept Comparison with the Performance of Cost and Risk

Based on the above reasoning, the box-beam concept design is selected within the specified control limits and performance specifications. The case study further demonstrates the parametric design refinement under the assistance of the representation of feasible space. The approach continues with the adoption of the product profit and failure risk as the system metrics.

The initial design, arbitrarily set at the middle point  $\mathbf{x}^0 = (55, 40, 3, 3)^T$ , is infeasible as indicated by its location outside of the local design space (identified as the darker regions) in Figure 11. It is trivial to acquire a feasible solution by observing the local design space and adjusting any of the parameters into the feasible region. While there are many options to achieve the feasible space, the designer, for the sake of argument, is assumed to decrease the middle thickness  $x_3$ ; Then the design vector becomes  $\mathbf{x}^1 = (55, 40, 0.9, 3)^T$ . The interface is updated in Figure 12. All the design parameters are now inside the updated local design space. Note that the global design space has not changed.

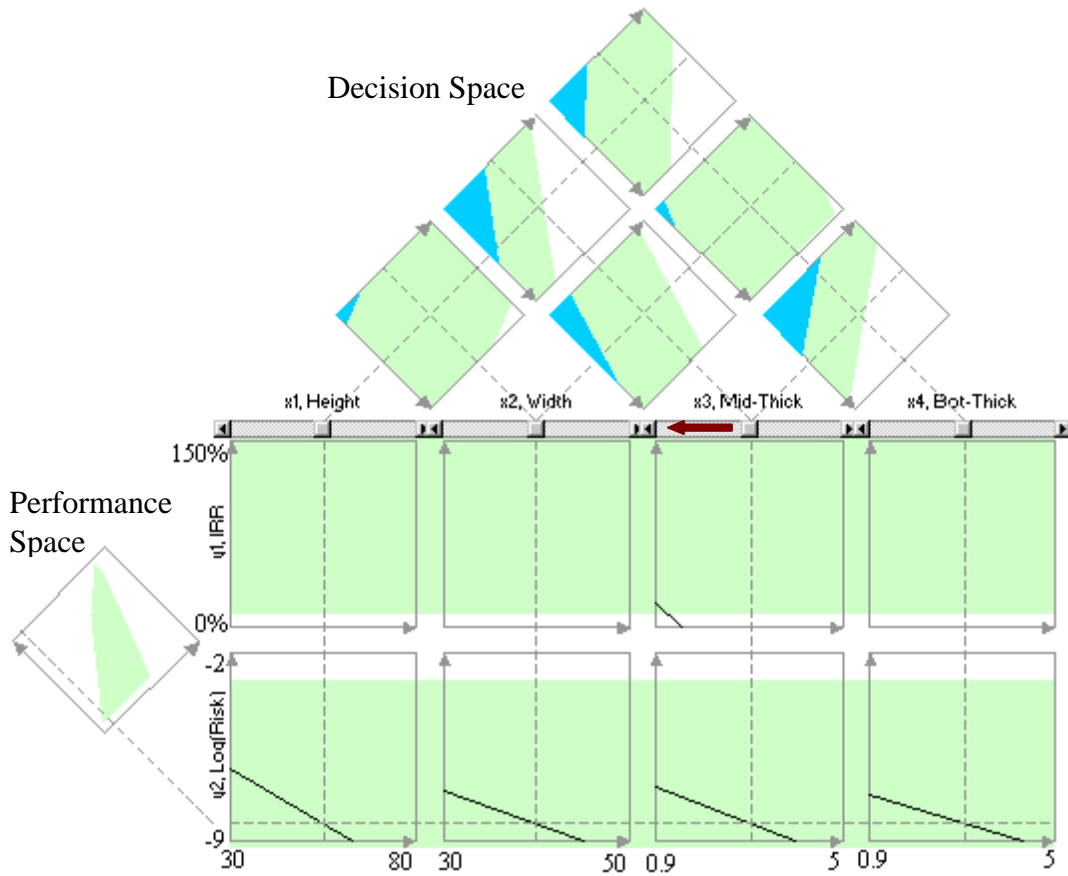


Figure 11: The Initial Interface of Beam Design with Feasible Space

The current design vector  $\mathbf{x}^1$  represents a feasible decision alternative, producing a beam design with 20% profit and 0.00001% failure risk. However, better system performance can be achieved by further refining the design parameters.

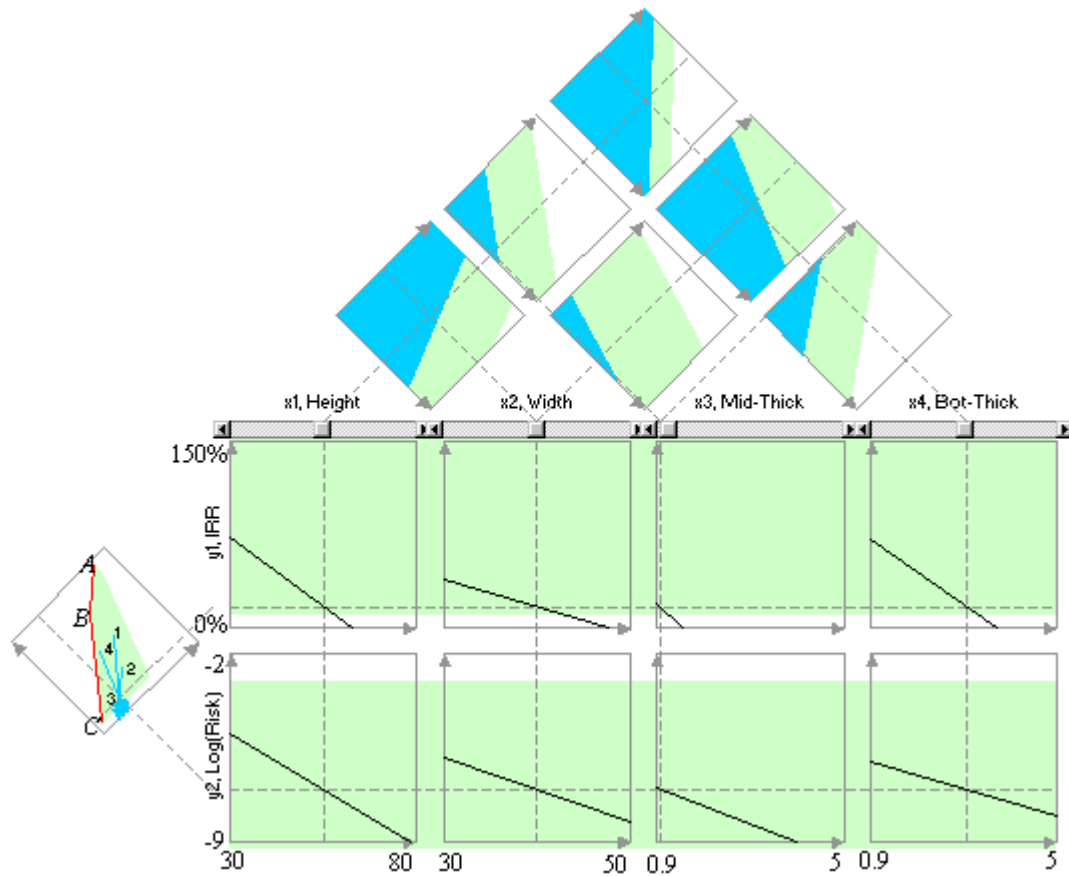


Figure 12: A Feasible Design Configuration

The boundary  $ABC$  in Figure 12 constitutes the Pareto optimal set. The extreme points  $A$ ,  $B$ , and  $C$  respectively corresponds to three performance attributes  $(1.45, 10^{-3})$ ,  $(1.06, 10^{-5.11})$ , and  $(0.10, 10^{-8.71})$ . In order to maximize the profit and minimize the risk, any design alternative on  $ABC$  will be an "optimal" solution. Since high reliability is expected for the airframe design, the designer may choose a design vector closer to the point  $C$ . Without loss of generality, it is assumed that the point  $B$  is desired. The labeled arrows lead the designer to decrease the bottom thickness  $x_4$ . Eventually, the point  $B$  is obtained with  $\mathbf{x}^B = (30, 50, 0.9, 0.9)$ . The performance space is updated in Figure 13. In addition, the higher profit could be captured by decreasing the width  $x_2$  as indicated by the parameter sensitivity arrows in the performance space.

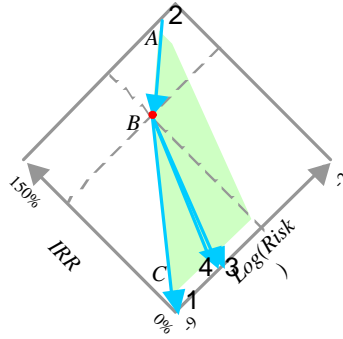


Figure 13: The Performance Trade-off in the Beam Design

It is worth noting that the active constraints of the extreme point  $A$ ,  $B$ , and  $C$  have been identified as  $A(\underline{x}_1, \underline{x}_3, \underline{x}_4, \bar{y}_2)$ ,  $B(\underline{x}_1, \bar{x}_2, \underline{x}_3, \underline{x}_4)$ , and  $C(\bar{x}_2, \underline{x}_3, \underline{x}_4, \underline{y}_1)$  based on the Extensive Simplex Method, in which  $\underline{x}$ ,  $\bar{x}$ ,  $\underline{y}$ , and  $\bar{y}$  are the upper and lower limits of the design parameters and performance attributes. Therefore, the Pareto optimal boundary could be improved by expanding  $\underline{x}_1$ ,  $\bar{x}_2$ ,  $\underline{x}_3$ , and  $\underline{x}_4$ . The complete constraint graph is shown in Figure 14 where  $A$ ,  $B$ , and  $C$  are highlighted. Furthermore, each constraint loop can be traced. For instance, the upper specification  $\bar{y}_2$  consists of the extreme point 1, 2, 3, and 5.

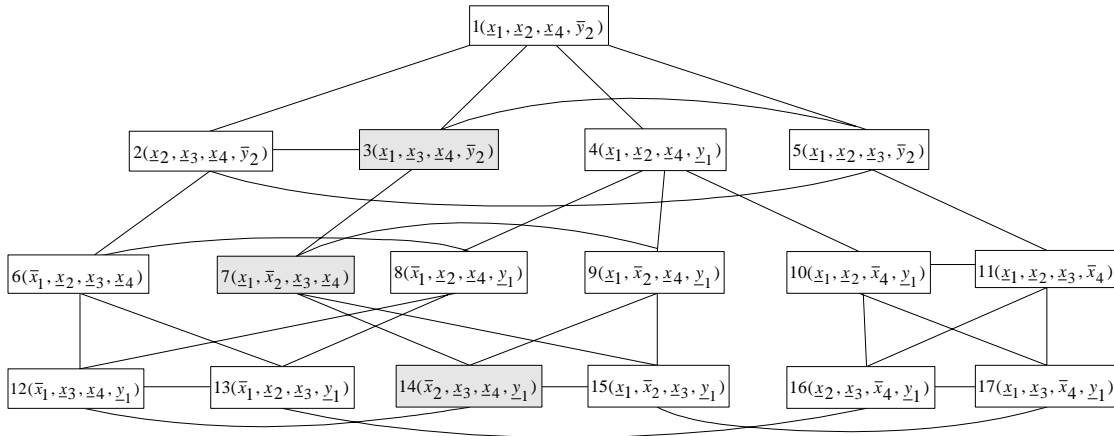


Figure 14: Active Constraints of Extreme Points

In addition, the inverse reasoning approach could be adopted to refine the design. For instance, the decision is made to raise the minimum profit to 50% and lower the maximum risk to  $10^{-6}$ . The updated representation is shown in Figure 15. With the much smaller design space, the designer can focus on the interested design range and obtain the desired solution. Alternatively, the designer may continue to narrow the performance requirements until only a single design exists. As indicated on the interface, the height,

middle-thickness, and bottom-thickness have been limited to the lower end of the specified ranges in order to satisfy the new performance requirements.

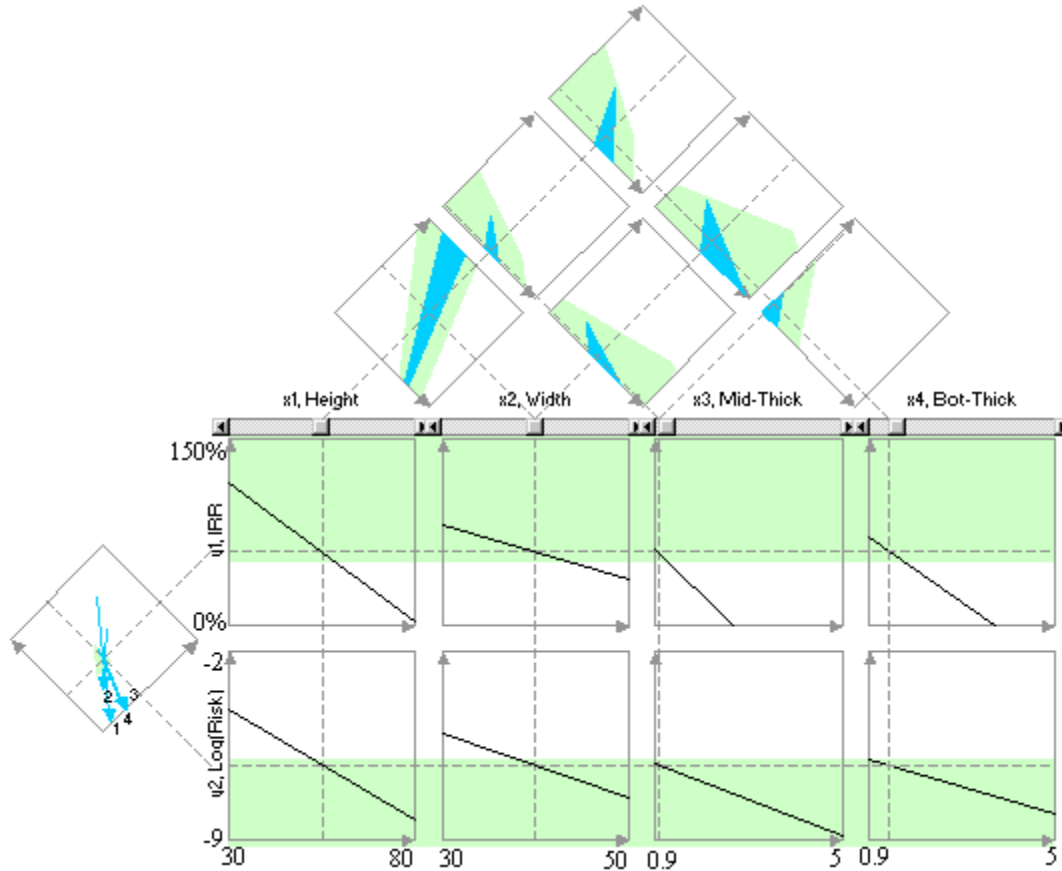


Figure 15: The Feasible Space with Restricted Specifications

## 5 Conclusion

A goal of system design is to select a set of design parameters to achieve the desired system performance. Theoretically, any design vector that satisfies all specifications is a feasible design. In reality, the initial specifications rarely reflect the ideal product requirements and are subject to frequent modifications during the subsequent stages of the design. Even when specifications are well defined, the customer would prefer the best compromise of all performance attributes. The conventional optimization approach does not provide enough assistance on these perspectives of design. The proposed representation is believed to be a useful tool in the synthesis of engineering decisions. The initial case study shows that the design interface of feasible space can help decision makers to quickly grasp an understanding of the design problem and its performance limitations. This understanding, together with the performance

inverse reasoning and parameter constraint space, leads directly to a better design decision. As such, the decision makers' confidence in the final design and their ability to modify the design given a changed specification are considerably improved.

The described representation of an evolving feasible space assists the synthesis of engineering decisions as illustrated in a beam design problem. Given two design concepts a set of initial specifications, the feasible performance space assists the designer in selecting the box-shape over the I-shape for the potential to provide higher profit and lower risk within the specified limits. The box-beam problem is further continued with parametric design. First, a feasible design is obtained within the local design space. Second, the system performance is improved by locating a design vector on the Pareto optimal boundary of the feasible performance space. The design sensitivity analysis also provides the decision basis for the further negotiation of multi-attribute trade-offs. Finally, the constraint identification and inverse reasoning reveal more insight to the design specifications of beam problem.

However, the methodology has limitations. First, its application is limited by poor fidelity of linear approximation. Piecewise linearization is a possible solution, but increases the problem dimensionality with increasing precision. More sophisticated case studies are required to further establish the significance of the methodology. Furthermore, the methodology should be extended to consider the effect of variation and model uncertainty in the synthesis of engineering designs.

### **Acknowledgement**

This research is supported by National Science Foundation, grant #9702797, through the Division of Design, Manufacture, and Industrial Innovation.

## References

1. Hazelrigg, G.A., *A Framework for Decision-Based Engineering Design*. Journal of Mechanical Design, 1998. 120(December): p. 653-658.
2. Neumann, J.v. and O. Morgenstern, *Theory of Games and Economic Behavior*. 3 ed. 1953: Princeton University Press. 641.
3. Luce, R.D. and H. Raiffa, *Games and Decisions*. 1957: John Wiley & Sons, Inc. 509.
4. Antonsson, E.K. and K.N. Otto, *Imprecision in Engineering Design*. ASME Journal of Mechanical Design, 1995, 117B, p. 25-32.
5. Bras, B. and F. Mistree, *A Compromise Decision Support Problem for Axiomatic and Robust Design*. ASME Journal of Mechanical Design, 1995. 117(1): p. 10-19.
6. Keeney, R.L., *Multiplicative Utility Functions*. Operations Research, 1974. 1: p. 22-34.
7. Thurston, D.L., *A Formal Method for Subjective Design Evaluation with Multiple Attributes*. Research in Engineering Design, 1991. 3: p. 105-122.
8. Iyer, H.V. and S. Krishnamurty. *A Preference Based Robust Design Metric*. in *Design ENgineering Technical Conference*. 1998. Atlanta, Georgia.
9. Yoshimura, M. and H. Kondo. *Group Decision Making in Product Design and Manufactruing*. in *Proceedings of the ASME Design Engineering Technical Conference*. 1997. Sacramento, California.
10. Tidd, W.F., J.R. Rinderle, and A. Witkin. *Design Refinement via Interactive Manipulation of Design Parameters and Behaviors*. in *Proceedings of the ASME Design Theory and Methodology Conference*. 1992. Scottsdale, Arizona.
11. Ramaswamy, R. and K. Ulrich, *A Designer's Spreadsheet*. ASME Journal of Mechanical Design, 1997. 119(March): p. 48-56.
12. Campbell, M.I., J. Cagan, and K. Kotovsky, *A-Design: An Agent-Based Approach to Conceptual Design in a Dynamic Environment*. Research in Engineering Design, 1999. 11(3): p. 172-192.
13. Chen, R. and A.C. Ward, *The RANGE family of propagation operations for intervals on simultaneous linear equations*. Artificial Intelligence for Engineering Design, Analysis and Manufacturing, 1995. 9(3): p. 183-196.
14. McAdams, D.A. and K. Wood, *Tuning Parameter Tolerance Design: Foundations, Methods, and Measures*. Research in Engineering Design, 2000. 12(3): p. 152-162.
15. Zhu, L. and D. Kazmer. *An Extensive Simplex Method Mapping the Global Feasibility*. in *ASME DETC the 28th Design Automation Conference*. 2002. Montreal, Canada, DETC2002/DAC-34115
16. Neter, J., et al., *Applied Linear Statistical Models*. 4 ed. 1996, Chicago: Irwin. 1408.
17. Allgower, E.L. and K. Georg, *Piecewise Linear Methods for Nonlinear Equations and Optimization*. Journal of Computational and Applied Mathematics, 2000. 124.

18. Dantzig, G.B., *Linear Programming and Extensions*. xvi ed. 1998: Princeton University Press. 627.
19. Chernikova, N.V., *Algorithm for Finding a General Formula for the Non-negative Solutions of a System of Linear Inequalities*. U. S. S. R. Computational Mathematics and Mathematical Physics, 1965. 5(2): p. 228-233.
20. Steuer, R.E., *Random Problem Generation and the Computation of Efficient Extreme Points in Multiple Objective Linear Programming*. Computational Optimization and Applications, 1994. 3: p. 333-347.
21. Ward, M.O. *XmdvTool: Integrating Multiple Methods for Visualizing Multivariate Data*. in *Proceedings of IEEE Conference on Visualization*. 1994.
22. Yin, H., *ViSOM -- A Novel Method for Multivariate Data Projection and Structure Visualization*. IEEE Transactions on Neural Networks, 2002. 13(1): p. 237-243.
23. Furnas, G.W., A. Buja, and Bellcore, *Prosection Views: Dimensional Inference through Sections and Projections*. Journal of Computational and Graphical Statistics, 1993. 3(4): p. 323-353.
24. Steuer, R.E., *Multiple Criteria Optimization: Theory, Computation, and Application*. 1986, New York: Wiley. 546.
25. Taguchi, G., *Robust technology development*. Mechanical Engineering, 1993. 115(3): p. 60-62.
26. Taguchi, G. and S. Konishi, *Taguchi Methods, Research and Development*. Quality engineering series. Vol. 1. 1992, Dearborn, Mich.: ASI Press. xvii, 351.
27. Kazmer, D., et al., *Definition and Application and A Process Flexibility Index*. ASME Journal of Manufacturing Systems, 2002, to appear.
28. Otto, K.N. and K.L. Wood. *Product Evolution: A reverse Engineering and Redesign Methodology*. in *Proceedings of ASME Design Theory and Methodology Conference*. 1996. Irvine, California,.
29. Osyczka, A., *Multicriteria Optimization for Engineering Design*, in *Design Optimization*. 1985.
30. Zhu, L. and D. Kazmer. *Comparing constraint based reasoning and decision based design in a performance-based representation*. in *Proceedings of ASME Design Engineering Technical Conference on Design Theory and Methodology*. 2000. Baltimore, Maryland, DETC2000/DTM-14556.